Rapid Communications

Interfacial mechanism in the anomalous Hall effect of Co/Bi_2O_3 bilayers

Edurne Sagasta,[1] Juan Borge,[2] Luis Esteban,[1] Yasutomo Omori,[3] Martin Gradhand,[4] YoshiChika Otani,[3,5] Luis E. Hueso,[1,6] and Fèlix Casanova[1,6]

[1]*CIC nanoGUNE, 20018 Donostia-San Sebastian, Basque Country, Spain*
[2]*Departamento de Física de Materiales, Universidad del País Vasco, Nano-Bio Spectroscopic Group, 20018 Donostia-San Sebastian, Basque Country, Spain*
[3]*Institute for Solid State Physics, University of Tokyo, Kashiwa, Chiba 277-8581, Japan*
[4]*H. H. Wills Physics Laboratory, University of Bristol, Bristol BS8 1TL, United Kingdom*
[5]*RIKEN-CEMS, 2-1 Hirosawa, Wako, Saitama 351-0198, Japan*
[6]*IKERBASQUE, Basque Foundation for Science, 48013 Bilbao, Basque Country, Spain*

(Received 27 March 2019; revised manuscript received 16 August 2019; published 18 September 2019)

Oxide interfaces are a source of spin-orbit coupling which can lead to novel spin-to-charge conversion effects. In this Rapid Communication, the contribution of the Bi_2O_3 interface to the anomalous Hall effect (AHE) of Co is experimentally studied in Co/Bi_2O_3 bilayers. We evidence a variation of ∼40% in the AHE of Co when a Bi_2O_3 capping layer is added to the ferromagnet. This strong variation is attributed to an additional source of asymmetric transport in Co/Bi_2O_3 bilayers that originates from the Co/Bi_2O_3 interface and contributes to the skew scattering.

DOI: 10.1103/PhysRevB.100.100407

Spin-orbit coupling (SOC), the interaction between the charge and spin degree of freedom of electrons, is the origin of many novel spin-dependent phenomena which are widely studied in the field of spin orbitronics [1,2]. Some particularly relevant for applications are the spin-charge current interconversions: The spin Hall effect (SHE) [3,4] occurs in the bulk of conductors, where SOC acts as an effective magnetic field that deflects the spin-up and spin-down electrons in the opposite direction, and the Edelstein effect [5] at Rashba interfaces [6,7] or surface states of topological insulators [8], where SOC generates a spin texture with spin-momentum locking.

In ferromagnetic (FM) metals, the SHE appears alongside the anomalous Hall effect (AHE) which, due to the unbalanced spin population, generates a transverse charge accumulation when a charge current (which is spin polarized) is applied to the system [9,10]. Depending on the origin of the SOC, we distinguish between the intrinsic [11] and extrinsic mechanisms [12,13]. In the first case, SOC is inherent to the band structure of the material and the intrinsic anomalous Hall conductivity (σ_{AH}^{int}) is determined by the Berry curvature. σ_{AH}^{int} thus depends on the crystallographic phase of the FM: For instance, different values were calculated for hcp Co and fcc Co by Roman *et al.*, which are in quite good agreement with experimental results [14]. For a given crystallographic phase, σ_{AH}^{int} is generally anisotropic; for instance, it is different for bcc Fe(001) and bcc Fe(111) [15,16]. In a system with less symmetries, more complex antisymmetric responses can be observed as the magnetization is changed [14,16]. *Ab initio* calculations suggest that σ_{AH}^{int} may also decrease when entering the dirty limit [17]. In the extrinsic case, the electrons feel an effective SOC induced by the presence of impurities in the lattice [9]. Among the extrinsic mechanisms we find the skew scattering and side jump, with the strength of each mechanism depending on the type of impurity and the host material [9,18–21].

It has been theoretically predicted that the inversion symmetry breaking at the interface of different materials generates giant SOC that can result in extra spin-charge interconversion effects in the bulk [22–25]. This prediction has been evidenced in the results of *ab initio* calculations, which show a large enhancement of the spin-charge interconversion, which is not confined to the interface between the two metals [26,27]. In this framework, it is appealing to unveil whether the inversion symmetry breaking introduced when a FM is interfaced with a nonmagnetic (NM) material, either metallic or insulating, can affect the AHE. Interestingly, the AHE has been observed to be modified in the presence of metallic interfaces [28,29].

In this Rapid Communication, we study the AHE in Co/Bi_2O_3 bilayers for different Co thicknesses, unraveling the role that the interface between Co and Bi_2O_3 plays in the AHE of Co. We consider Bi_2O_3 an ideal material since (i) due to its insulating nature, we can discard additional effects such as extra magnetoresistances coming from the NM layer, and (ii) a large Rashba coefficient is expected in our Co/Bi_2O_3 system, as the work function of Co is similar to that of Cu [30,31]. A strong variation of the AHE is observed by adding the Bi_2O_3 capping layer to the Co. The temperature dependence of the AHE allows us to extract the weight of the intrinsic and extrinsic contributions. We observe that the intrinsic contribution is insensitive to the Bi_2O_3 capping layer, demonstrating that no Rashba contribution modifies the intrinsic contribution. Interestingly, it decreases with increasing the residual resistivity of Co, as predicted theoretically when the system enters the dirty regime [17]. In contrast, the Bi_2O_3 capping layer acts as a scattering source at the interface, with a contribution to the observed skew scattering that decays with the thickness of the Co layer.

All Co and Co/Bi_2O_3 thin films were deposited *in situ* on top of doped Si/SiO_2 (150 nm) substrates. Co was *e*-beam

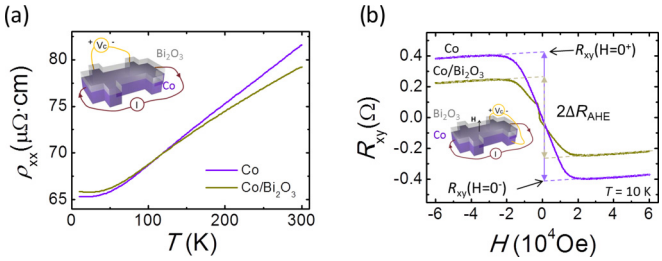

FIG. 1. (a) Temperature dependence of the longitudinal resistivity of Co(10) (purple line) and Co(10)/Bi_2O_3 (golden line). Inset: Measurement configuration of the longitudinal resistivity. (b) Anomalous Hall effect measurement in Co(10) (purple line) and Co(10)/Bi_2O_3 (golden line) at 10 K. Dashed lines are linear curves fitted to high magnetic field data. The intercept of the fit at positive (negative) magnetic fields defines $R_{xy}(H = 0^+)[R_{xy}(H = 0^-)]$, as indicated for the purple line that corresponds to Co reference. Inset: Measurement configuration of the transverse resistivity applying out-of-plane magnetic field. The applied current I is 1 μA in (a) and 10 μA in (b).

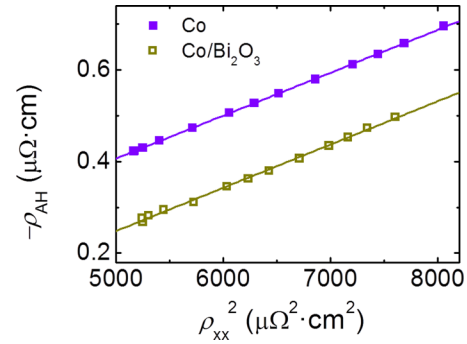

FIG. 2. Anomalous Hall resistivity as a function of the square of the longitudinal resistivity of Co (solid purple squares) and Co/Bi_2O_3 (open golden squares). Purple solid line (golden solid line) is the fitting of Co (Co/Bi_2O_3) data to Eq. (1).

evaporated at 0.5 Å/s and $\sim 8 \times 10^{-7}$ Torr and Bi_2O_3 was also e-beam evaporated at 0.1 Å/s and $\sim 2 \times 10^{-6}$ Torr in all the samples. The 100-μm-wide and 780-μm-long Hall bars were patterned by negative photolithography and subsequent ion milling was performed. The thickness of Bi_2O_3 is 20 nm for all the Co(t)/Bi_2O_3 bilayers and the thickness of Co, t, varies from 10 to 160 nm. The grazing incidence x-ray diffraction spectrum shows, for all the samples, a broad and low peak at $\sim 44.5^\circ$ that corresponds to (0002) hcp Co, indicating that the films consist of small grains of hcp Co with preferential orientation of the c axis out of plane [32]. We cannot confirm whether other orientations are also present out of plane, as the corresponding peak might be unresolvable. Longitudinal [inset in Fig. 1(a)] and transverse [inset in Fig. 1(b)] magneto-transport measurements were carried out using a "dc reversal" technique [33] in a liquid-He cryostat, applying an external magnetic field H and varying temperature T.

The longitudinal resistivity ρ_{xx} as a function of temperature of the Co(t) reference layers and Co(t)/Bi_2O_3 bilayers overlaps, as expected from Bi_2O_3 being an insulator. An example is shown in Fig. 1(a) for 10-nm-thick Co. The transverse resistance, $R_{xy} = V_c/I$, is measured in the Co(t) reference Hall bars and Co(t)/Bi_2O_3 bilayer Hall bars as a function of the external out-of-plane magnetic field at different temperatures. Figure 1(b) shows the case for a Co thickness of 10 nm at 10 K. At $|H| \gtrsim 2$ T, where the magnetization of Co is saturated out of plane, there is a linear dependence of R_{xy} with H in both systems, due to the ordinary Hall effect occurring in Co. Namely, the slopes are the same for Co and Co/Bi_2O_3, indicating that the current is flowing through Co in both systems and the density of charge carriers does not change from the reference to the bilayer. At $|H| \lesssim 2$ T, we evidence the magnetization rotation. Importantly, the jump of the transverse resistance from positive values to negative values, which is associated with the AHE and is quantified as $2\Delta R_{AHE}$ [see Fig. 1(b)], varies from the Co reference sample to the sample with the Bi_2O_3 capping. For the case shown in Fig. 1(b), a remarkable $\sim$40% decrease is observed. The large variation in the AHE cannot be attributed to a change in ρ_{xx} of Co, which is very close for the two samples [Fig. 1(a)], and, hence, the effect is arising from the presence of the Bi_2O_3 capping. This clearly indicates that, in Co(10)/Bi_2O_3, in addition to the regular AHE occurring in the bulk of FM, there is an extra contribution to the AHE.

To extract $2\Delta R_{AHE}$, we fit the data at high positive and negative magnetic fields to two linear functions [see the dashed lines in Fig. 1(b)]. From the intercept of the fittings at high positive and negative magnetic fields we obtain $R_{xy}(H = 0^+)$ and $R_{xy}(H = 0^-)$, respectively. The difference between the two values gives $2\Delta R_{AHE}$ and the anomalous Hall resistivity is calculated by $\rho_{AH} = t\,\Delta R_{AHE}$. We extract ρ_{AH} for both systems at different temperatures. By following the empirical relation for the AHE proposed by Tian *et al.* [34] that considers both the extrinsic (skew scattering and side jump) and intrinsic contributions to the AHE of Co, we can write the anomalous Hall resistivity as

$$-\rho_{AH} = \sigma_{AH}^{int}\rho_{xx}^2 + \alpha_{AH}^{ss}\rho_{xx0} + \sigma_{AH}^{sj}\rho_{xx0}^2, \quad (1)$$

where σ_{AH}^{int} is the intrinsic anomalous Hall conductivity, α_{AH}^{ss} is the skew scattering angle, σ_{AH}^{sj} is the anomalous Hall conductivity that corresponds to the side jump contribution, and ρ_{xx0} is the residual resistivity, the resistivity value measured at 10 K. The last two terms represent the extrinsic contribution,

$$-\rho_{AH}^{ext} = \alpha_{AH}^{ss}\rho_{xx0} + \sigma_{AH}^{sj}\rho_{xx0}^2. \quad (2)$$

Figure 2 shows ρ_{AH} as a function of the square of the longitudinal resistivity of Co for the Co(10) reference sample and the Co(10)/Bi_2O_3 bilayer. We clearly observe that the slopes of both curves are the same, 93.6 $\pm$ 0.6 and 94 $\pm$ 1 Ω^{-1} cm^{-1}, respectively, indicating that σ_{AH}^{int} is not affected by the Bi_2O_3 capping layer on top. However, we obtain a very different extrinsic contribution for each system. ρ_{AH}^{ext} in Co(10)/Bi_2O_3 (0.22 $\mu\Omega$ cm) is almost four times larger than in Co(10) (0.06 $\mu\Omega$ cm), demonstrating that the Co/Bi_2O_3 interface acts as an extrinsic scattering source.

Once the interfacial and extrinsic origin is demonstrated, we additionally calculate ρ_{AH} in Co(t) reference samples and Co(t)/Bi_2O_3 bilayers with different Co thicknesses, t = 10, 13, 16, 23, 39, 74, and 157 nm, not only as further supporting evidence of these origins, but to unravel which type of

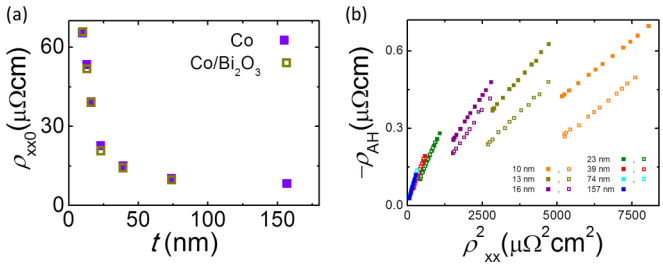

FIG. 3. (a) Residual resistivity of Co as a function of the thickness for the Co reference layers (solid purple squares) and the Co/Bi_2O_3 bilayers (open golden squares) at 10 K. (b) Anomalous Hall resistivity as a function of the square of the longitudinal resistivity of Co (solid squares) and Co/Bi_2O_3 (open squares) for different Co thicknesses. The applied currents range from 1 to 10 μA in (a) and from 10 to 100 μA in the measurements that gave the results shown in (b).

extrinsic mechanism, skew scattering or side jump, is driving the effect. The resistivity of Co for the Co(t) reference samples and Co(t)/Bi_2O_3 bilayers with the same Co thickness is the same, as shown in Fig. 3(a) at 10 K. We observe that the residual resistivity varies when the thickness of the Co layer is changed. Namely, it shows a t^{-1} dependence, following the Mayadas and Shatzkes model [35]. Figure 3(b) shows the anomalous Hall resistivity for all the samples with different Co thicknesses, with and without the Bi_2O_3 capping layer. Interestingly, the thinnest Co samples show a larger difference between the AHE signals with and without the Bi_2O_3 capping, further suggesting that the additional effect has an interfacial origin. We extract the weight of each mechanism (σ_{AH}^{int} and ρ_{AH}^{ext}) by fitting each individual sample to Eq. (1) as we did previously with $t = 10$ nm in Fig. 2.

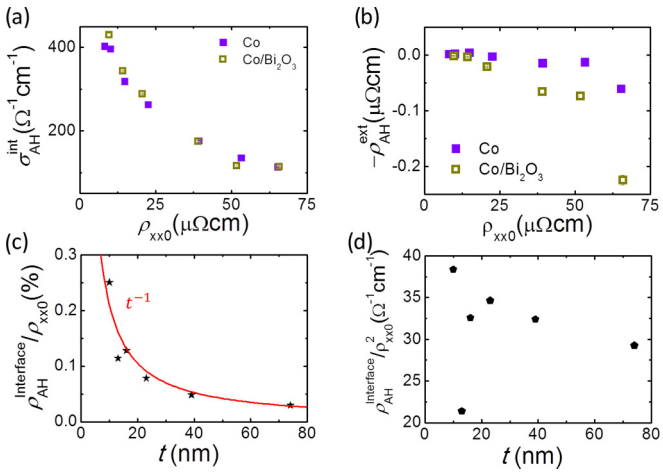

FIG. 4. Residual resistivity dependence of (a) the intrinsic anomalous Hall conductivity and (b) the extrinsic anomalous Hall resistivity of Co for the Co reference layers (solid purple squares) and the Co/Bi_2O_3 bilayers (open golden squares). (c) Thickness dependence of the ratio of the additional anomalous Hall resistivity at the interface and the residual resistivity of Co. Red solid line is a fit to t^{-1}. (d) Thickness dependence of the ratio of the additional anomalous Hall resistivity at the interface and the square of the residual resistivity of Co.

Figure 4(a) shows the intrinsic anomalous Hall conductivity σ_{AH}^{int}, obtained from the individual fitting for each sample, as a function of its residual resistivity. There is almost no difference between σ_{AH}^{int} obtained for the Co(t)/Bi_2O_3 bilayer and Co(t) reference samples, which is consistent with the result in Fig. 2. Therefore, we confirm that σ_{AH}^{int} in Co is independent of the presence of Bi_2O_3 capping layer on top. Taking into account that σ_{AH}^{int} is a property of the band structure of the material, this result indicates that the Bi_2O_3 capping layer is not modifying the band structure of Co.

Interestingly, the same results show that σ_{AH}^{int} is modified by the residual resistivity of Co, a feature in principle not expected. For instance, a constant σ_{AH}^{int} value of 205 Ω^{-1} cm^{-1} for hcp Co is reported for a residual resistivity range of $16 - 42\,\mu\Omega$ cm [36], while the σ_{AH}^{int} value we obtain for that resistivity range ($15 - 39\,\mu\Omega$ cm) decays from 318 to 176 Ω^{-1} cm^{-1}. However, our data are in good agreement with the tight-binding calculations performed by Naito *et al.* [17], which show a decay in σ_{AH}^{int} as the impurity concentration increases even before entering the dirty limit. They report a value of 341 Ω^{-1} cm^{-1} for Co with a residual resistivity of 5 $\mu\Omega$ cm, which decreases to 148 Ω^{-1} cm^{-1} before entering the dirty limit [17]. In our case, we obtain $402 \pm 4\,\Omega^{-1}$ cm^{-1} for 8.2 $\mu\Omega$ cm, which decays to $113.0 \pm 0.4\,\Omega^{-1}$cm^{-1} when the residual resistivity increases to 65.3 $\mu\Omega$ cm. This agreement suggests that we are experimentally observing the predicted decay of σ_{AH}^{int} as the residual resistivity increases in the intermediate (moderately dirty) regime of Co. An alternative explanation could be that the texture of the hcp Co varies with the thickness of Co, going from a c-axis orientation of the grains to an *ab*-plane orientation. As reported by Roman *et al.*, σ_{AH}^{int} for hcp Co in the c axis is 481 Ω^{-1}cm^{-1} and in the *ab* plane is 116 Ω^{-1} cm^{-1} [14], values that would be in agreement with our results. However, we cannot resolve any variation in the texture of our polycrystalline Co films from the x-ray diffraction measurements.

We now turn to the extrinsic contribution ρ_{AH}^{ext}, obtained from the individual fitting for each sample. ρ_{AH}^{ext} differs significantly from the reference sample to the bilayer system [see Fig. 4(b)]. Figures 4(a) and 4(b) clearly confirm the conclusion of Fig. 2: For all pairs of samples, the intrinsic contribution is constant and the extrinsic one is changed when the Bi_2O_3 capping layer is added. Together with Figs. 1(a) and 3(a), which highlight that the residual resistance is not changing by the capping and thus restricting any possible effect to the interface, we can confirm the interfacial and extrinsic origin of the additional effect. Next, we can proceed to analyze the ρ_{AH}^{ext} data set.

We first analyze ρ_{AH}^{ext} in the reference samples, which corresponds to the bulk of Co, in order to disentangle the skew scattering from the side jump contributions. By plotting $-\rho_{AH}^{ext}/\rho_{xx0}$ as a function of ρ_{xx0}, we can linearly fit the data to Eq. (2) in order to extract σ_{AH}^{sj} from the slope and α_{AH}^{ss} from the intercept. We obtain $\sigma_{AH}^{sj} = -17 \pm 3\ \Omega^{-1}$ cm^{-1} and $\alpha_{AH}^{ss} = 0.04 \pm 0.01\%$ for the Co reference samples. This extrinsic contribution from the bulk of the Co layer should also be present in the bilayer system. Therefore, in order to isolate the additional extrinsic contribution that is present only in the bilayer system due to the interface, we subtract ρ_{AH}^{ext} for

the corresponding Co reference layer from ρ_{AH}^{ext} of each bilayer, obtaining $\rho_{AH}^{interface}$. This interfacial extrinsic effect could modify either the skew scattering or the side jump. Conventionally, in a homogeneous bulk sample, the dependence of the skew scattering part of the extrinsic contribution is $\rho_{AH} = \alpha_{AH}^{ss}\rho_{xx0}$, where α_{AH}^{ss} is the coefficient that gives the strength of the skew scattering mechanism independent of ρ_{xx0} and for the side jump it would be $\rho_{AH} = \sigma_{AH}^{sj}\rho_{xx0}^2$, where σ_{AH}^{sj} is the coefficient that gives the strength of the side jump mechanism again independent of ρ_{xx0} [see Eq. (2)]. While these coefficients are constant for a given material with a homogeneous distribution of impurities, a t^{-1} dependence can be expected for the coefficient that is influenced by the interface. This dependence is the consequence of the extra scattering contribution originated at the interface in a diffusive system (i.e., mean free path$\ll t$). In order to resolve this question, we plot the characteristic coefficients of each mechanism, $\rho_{AH}^{interface}/\rho_{xx0}$ and $\rho_{AH}^{interface}/\rho_{xx0}^2$ for skew scattering and side jump, respectively, as a function of t [see Figs. 4(c) and 4(d)]. Any t dependence in $\rho_{AH}^{interface}$ coming from ρ_{xx0} is removed once we consider the adequately defined coefficients. Indeed, Fig. 4(c) shows that the ratio between $\rho_{AH}^{interface}$ and ρ_{xx0} follows a t^{-1} dependence, indicating that the interfacial contribution can be written as $\rho_{AH}^{interface} = \alpha_{AH}^{ss,interface}\rho_{xx0}$, where $\alpha_{AH}^{ss,interface}$ shows a t^{-1} dependence. In contrast, the ratio between $\rho_{AH}^{interface}$ and ρ_{xx0}^2 does not show any clear dependence with t [see Fig. 4(d)], which is not expected if the effect is generated at the interface. One could argue that the observed behavior is an additional side jump mechanism originating homogeneously along the thickness of the Co, but such a possibility could only occur if impurities from the capping layer are diffused into the Co layer for all thicknesses, which is fully incompatible with the observation of a constant residual resistivity when adding the capping layer. Therefore, we conclude that the interface modification, by adding a Bi_2O_3 layer on top of Co, results in an interfacial skew scattering contribution of the AHE in Co. Xu *et al.* reported an interfacial skew scattering in epitaxially grown Ni/Cu metallic bilayers, where $\alpha_{AH}^{ss,interface}$ is constant and does not depend on the thickness of Ni [28]. In contrast to our case, transport in their system is not in the diffusive regime along the thickness because their samples were grown epitaxially and the mean free path is longer than the thickness. A recently reported interface-induced anomalous Hall conductivity [37] is unlikely to be present in our system, given that our samples are polycrystalline.

To conclude, we evidence a variation of up to ~40% in the AHE of Co originated by interface modification. The addition of an insulating Bi_2O_3 layer on top of Co gives rise to interfacial skew scattering, where the skew scattering angle follows a t^{-1} dependence, characteristic of an interfacial effect. We also observe that the intrinsic anomalous Hall conductivity of Co is insensitive to the presence of the Bi_2O_3 capping layer. σ_{AH}^{int} decreases when we increase the residual resistivity in Co, evidencing the influence of the impurities of the bulk of Co on the intrinsic mechanism when the system enters the dirty limit.

We thank Vitaly N. Golovach and F. Sebastian Bergeret for useful discussions. This work is supported by the Spanish MINECO under the Maria de Maeztu Units of Excellence Programme (MDM-2016-0618) and under Projects No. MAT2015-65159-R, No. FIS2016-79464-P, and No. RTI2018-094861-B-100, and by the Japanese Grant-in-Aid for Scientific Research on Innovative Area, "Nano Spin Conversion Science" (Grant No. 26103002). E.S. thanks the Spanish MECD for support through a Ph.D. fellowship (Grant No. FPU14/03102). Y. Omori acknowledges financial support from JSPS through "Research Program for Young Scientists" and "Program for Leading Graduate Schools (MERIT). J.B. acknowledges financial support from the European Research Council (ERC-2015-AdG-694097).

[1] A. Soumyanarayanan, N. Reyren, A. Fert, and C. Panagopoulos, Nature (London) **539**, 509 (2016).
[2] A. Manchon, H. C. Koo, J. Nitta, S. M. Frolov, and R. A. Duine, Nat. Mater. **14**, 871 (2015).
[3] A. Hoffmann, IEEE Trans. Magn. **49**, 5172 (2013).
[4] J. Sinova, S. O. Valenzuela, J. Wunderlich, C. H. Back, and T. Jungwirth, Rev. Mod. Phys. **87**, 1213 (2015).
[5] V. M. Edelstein, Solid State Commun. **73**, 233 (1990).
[6] J. C. Rojas Sánchez, L. Vila, G. Desfonds, S. Gambarelli, J. P. Attané, J. M. De Teresa, C. Magén, and A. Fert, Nat. Commun. **4**, 2944 (2013).
[7] M. Isasa, M. C. Martinez-Velarte, E. Villamor, C. Magen, L. Morellon, J. M. De Teresa, M. R. Ibarra, G. Vignale, E. V. Chulkov, E. E. Krasovskii, L. E. Hueso, and F. Casanova, Phys. Rev. B **93**, 014420 (2016).
[8] J.-C. Rojas-Sánchez, S. Oyarzún, Y. Fu, A. Marty, C. Vergnaud, S. Gambarelli, L. Vila, M. Jamet, Y. Ohtsubo, A. Taleb-Ibrahimi, P. Le Fèvre, F. Bertran, N. Reyren, J.-M. George, and A. Fert, Phys. Rev. Lett. **116**, 096602 (2016).
[9] N. Nagaosa, J. Sinova, S. Onoda, A. H. MacDonald, and N. P. Ong, Rev. Mod. Phys. **82**, 1539 (2010).
[10] Y. Omori, E. Sagasta, Y. Niimi, M. Gradhand, L. E. Hueso, F. Casanova, and Y. C. Otani, Phys. Rev. B **99**, 014403 (2019).
[11] R. Karplus and J. M. Luttinger, Phys. Rev. **95**, 1154 (1954).
[12] J. Smit, Physica **24**, 39 (1958).
[13] L. Berger, Phys. Rev. B **2**, 4559 (1970).
[14] E. Roman, Y. Mokrousov, and I. Souza, Phys. Rev. Lett. **103**, 097203 (2009).
[15] L. Wu, Y. Li, J. Xu, D. Hou, and X. Jin, Phys. Rev. B **87**, 155307 (2013).
[16] M. Seemann, D. Kodderitzsch, S. Wimmer, and H. Ebert, Phys. Rev. B **92**, 155138 (2015).
[17] T. Naito, D. S. Hirashima, and H. Kontani, Phys. Rev. B **81**, 195111 (2010).
[18] B. Zimmermann, K. Chadova, D. Kodderitzsch, S. Blugel, H. Ebert, D. V. Fedorov, N. H. Long, P. Mavropoulos, I. Mertig, Y. Mokrousov, and M. Gradhand, Phys. Rev. B **90**, 220403(R) (2014).
[19] F. Topler, A. Honemann, K. Tauber, D. V. Fedorov, M. Gradhand, I. Mertig, and A. Fert, Phys. Rev. B **94**, 140413(R) (2016).

[20] A. Fert and P. M. Levy, Phys. Rev. Lett. **106**, 157208 (2011).
[21] K. Chadova, D. V. Fedorov, C. Herschbach, M. Gradhand, I. Mertig, D. Ködderitzsch, and H. Ebert, Phys. Rev. B **92**, 045120 (2015).
[22] I. V. Tokatly, E. E. Krasovskii, and G. Vignale, Phys. Rev. B **91**, 035403 (2015).
[23] J. Borge and I. V. Tokatly, Phys. Rev. B **96**, 115445 (2017).
[24] J. Borge and I. V. Tokatly, Phys. Rev. B **99**, 241401(R) (2019).
[25] V. P. Amin and M. D. Stiles, Phys. Rev. B **94**, 104419 (2016).
[26] S. Li, K. Shen, and K. Xia, Phys. Rev. B **99**, 134427 (2019).
[27] L. Wang, R. J. H. Wesselink, Y. Liu, Z. Yuan, K. Xia, and P. J. Kelly, Phys. Rev. Lett. **116**, 196602 (2016).
[28] J. Xu, Y. Li, D. Hou, L. Ye, and X. Jin, Appl. Phys. Lett. **102**, 162401 (2013).
[29] Y. Q. Zhang, N. Y. Sun, W. R. Che, R. Shan, and Z. G. Zhu, AIP Adv. **6**, 025214 (2016).
[30] S. Karube, K. Kondou, and Y. Otani, Appl. Phys. Express **9**, 033001 (2016).
[31] H. Tsai, S. Karube, K. Kondou, N. Yamaguchi, F. Ishii, and Y. Otani, Sci. Rep. **8**, 5564 (2018).
[32] L. Fallarino, O. Hovorka, and A. Berger, Phys. Rev. B **94**, 064408 (2016).
[33] E. Sagasta, Y. Omori, M. Isasa, Y. Otani, L. E. Hueso, and F. Casanova, Appl. Phys. Lett. **111**, 082407 (2017).
[34] Y. Tian, L. Ye, and X. Jin, Phys. Rev. Lett. **103**, 087206 (2009).
[35] A. F. Mayadas and M. Shatzkes, Phys. Rev. B **1**, 1382 (1970).
[36] J. Kötzler and W. Gil, Phys. Rev. B **72**, 060412(R) (2005).
[37] O. E. Parfenov, D. V. Averyanov, A. M. Tokmachev, I. A. Karateev, A. N. Taldenkov, O. A. Kondratev, and V. G. Storchak, ACS Appl. Mater. Interfaces **10**, 35589 (2018).